Supporting Information

Regulating disordered plasmonic nanoparticles into polarization sensitive metasurfaces

Shulei Li,[1] Mingcheng Panmai,[1] Shaolong Tie,[2] Yi Xu,[3] Jin Xiang[4] and Sheng Lan[1,*]

[1] Guangdong Provincial Key Laboratory of Nanophotonic Functional Materials and Devices, School of Information and Optoelectronic Science and Engineering, South China Normal University, Guangzhou, China

[2] School of Chemistry, South China Normal University, Guangzhou, China

[3] Department of Electronic Engineering, College of Information Science and Technology, Jinan University, Guangzhou, China

[4] Department of Electrical and Computer Engineering, University of Wisconsin–Madison, Madison, USA

*E-mail: slan@scnu.edu.cn

Supplementary Note 1: Morphology of Au nanoislands formed on the surface of the polymer film

The two-dimensional closely-packed Au nanoislands used in this work were obtained by sputtering Au on a polymer (PMMA) film. The morphology of Au nanoislands depends strongly on the sputtering time. We fabricated Au nanoislands with different morphologies by controlling the sputtering time and closely-packed Au nanoislands could be achieved by using a sputtering time longer than 15 s. The transmission electron microscope (TEM) images of the closely-packed Au nanoislands fabricated at different sputtering times are shown in Figure S1.

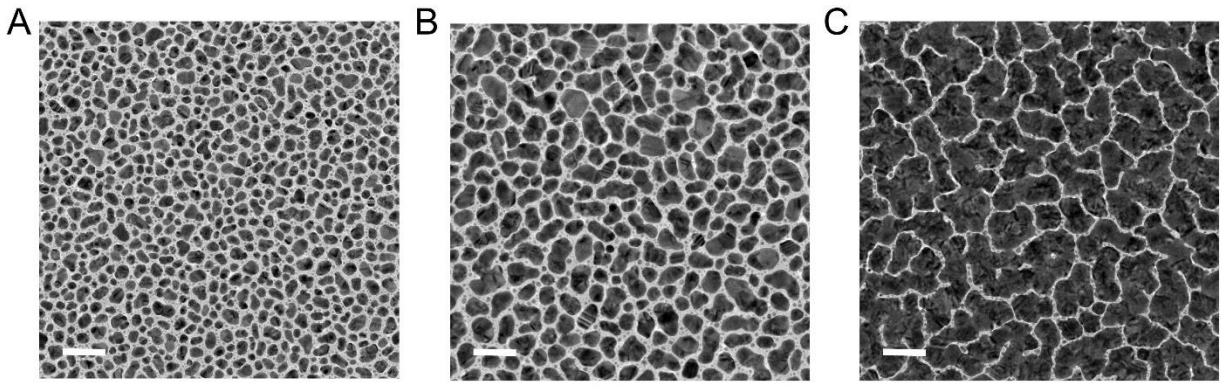

Figure S1. TEM images of closely–packed Au nanoislands obtained by using different sputtering times of 20 s (A), 30 s (B), and 40 s (C). The length of the scale bar is 100 nm.

Supplementary Note 2: Morphology of Au nanoislands upon the irradiation of femtosecond laser light with increasing fluence

We examined the morphology evolution of two-dimensional closely-packed Au nanoislands upon the irradiation of femtosecond laser pulses with increasing fluence by using SEM observations, as shown in Figure S2A-D. Based on the SEM images, we also performed statistics for the size distribution of Au nanoparticles in different stages by using a software to extract the area of each Au nanoparticle in the image. A broadening of the size distribution was observed with increasing laser fluence, as shown in Figure S2E-H.

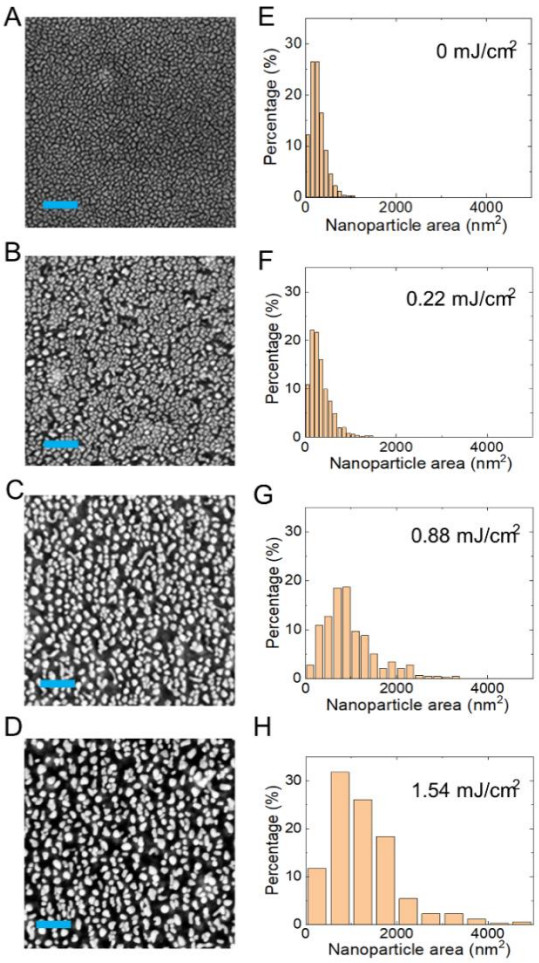

Figure S2. SEM images of two-dimensional closely-packed Au nanoislands upon the irradiation of femtosecond laser pulses with increasing fluence. (A) 0 mJ/cm^2, (B) 0.22 mJ/cm^2, (C) 0.88 mJ/cm^2, and (D) 1.54 mJ/cm^2. The length of the scale bar is 200 nm. The corresponding statistics of the size distribution of Au nanoparticles in different stages are presented in (E)–(H), respectively.

Supplementary Note 3: Structural colors exhibited by nanogratings fabricated and illuminated under different conditions

In our experiments, we irradiated closely-packed Au nanoislands on the surface of a sample by using femtosecond laser pulses with different polarizations and fluence. The morphology changes of closely-packed Au nanoislands induced by femtosecond laser pulses lead to various structural

colors which exhibit strong dependences on the polarization and fluence of the femtosecond laser light as well as the polarization of the incident white light, as shown in Figure S3.

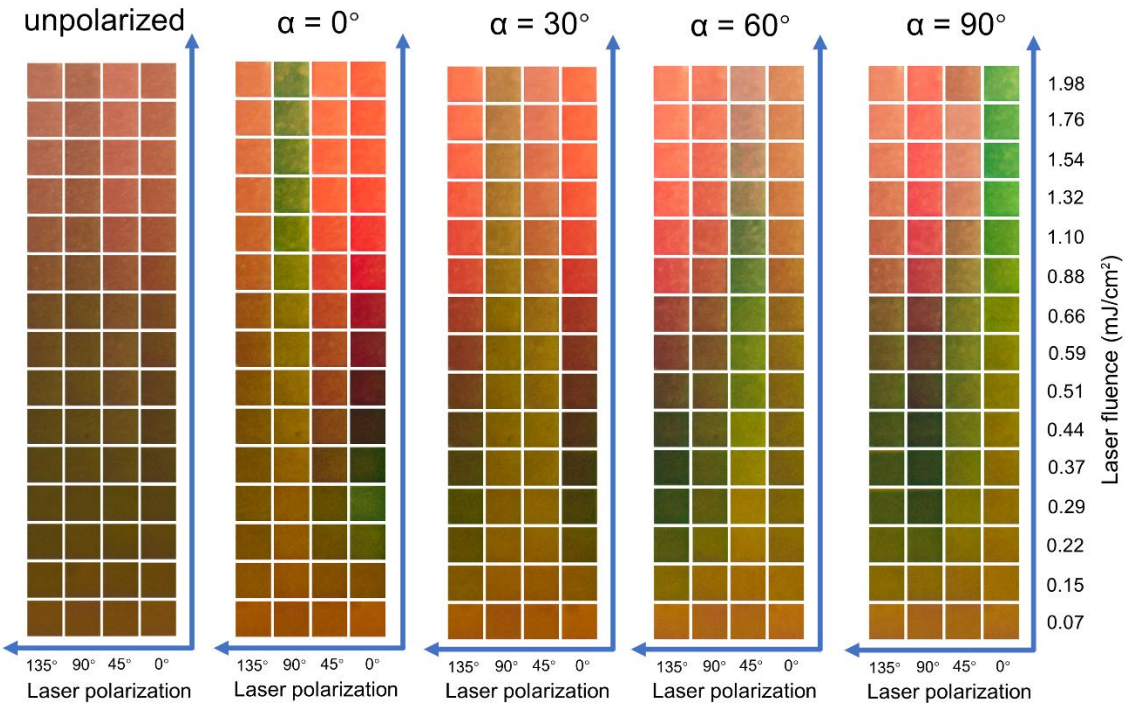

Figure S3 Structural colors observed by illuminating the nanogratings, which are fabricated by using femtosecond laser pulses with different polarization angles (0°, 45°, 90°, and 135°) and different fluence (0.07–1.98 mJ/cm^2), with unpolarized white light and polarized white light with different polarization angles of 0°, 30°, 60°, and 90°.

Supplementary Note 4: Color indices derived for the structural colors exhibited by nanogratings

We calculated the color indices for the structural colors exhibited by the nanogratings based on the measured reflection spectra and plotted them in a color diagram (CIE 1931), as shown in Figure S4. It is noticed that the color indices located mainly on the green, yellow, and red regimes of the color diagram.

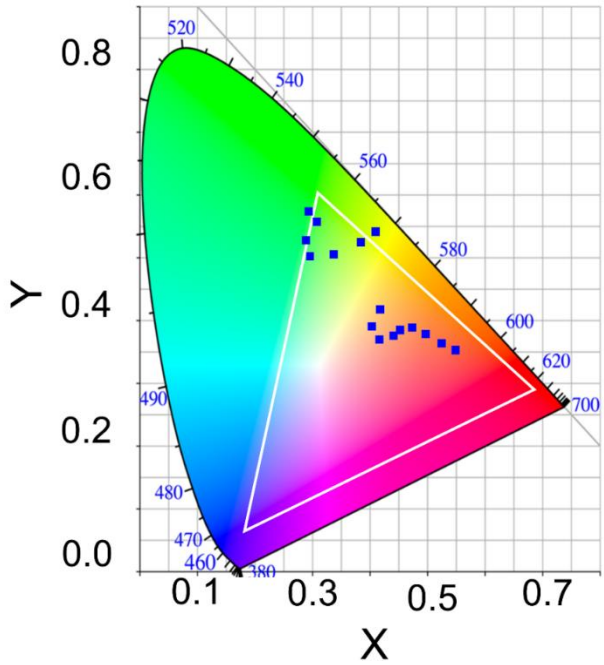

Figure S4. Color indices calculated for the structural colors exhibited by nanogratings based on their reflection spectra. Also shown is the RGB triangle.

Supplementary Note 5: Dependence of the structural color exhibited by nanogratings on the wavelength of femtosecond laser light

As shown in Supplementary Note 2, the morphology of closely-packed Au nanoislands depends strongly the laser fluence. As a result, the various structural colors can be obtained by using femtosecond laser light with different fluence, as shown in Figure 2A. In experiments, we also examined the influence of the laser wavelength on the structural color by using femtosecond laser light at different wavelengths of 750, 800, and 850 nm, as shown in Figure S5. It is noticed that the structural color is not sensitive to the laser wavelength at low laser fluence. However, it becomes highly dependent on the laser wavelength at high laser fluence owing to the formation of nanogratings. This unique feature can be exploited to realize wavelength multiplexing in optical data storage, as demonstrated in this work.

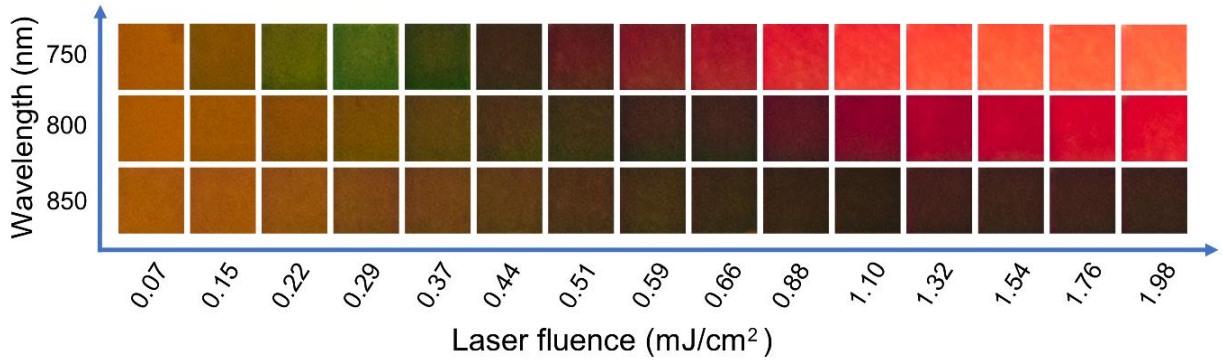

Figure S5. Color palettes obtained by irradiating the sample surfaces with femtosecond laser light of different wavelengths and fluence.

Supplementary Note 6: White light source used in the measurements

In the experiments described in this work, we used a halogen lamp with or without a polarizer as the illumination white light source. The spectrum of the halogen lamp was provided in Figure S6.

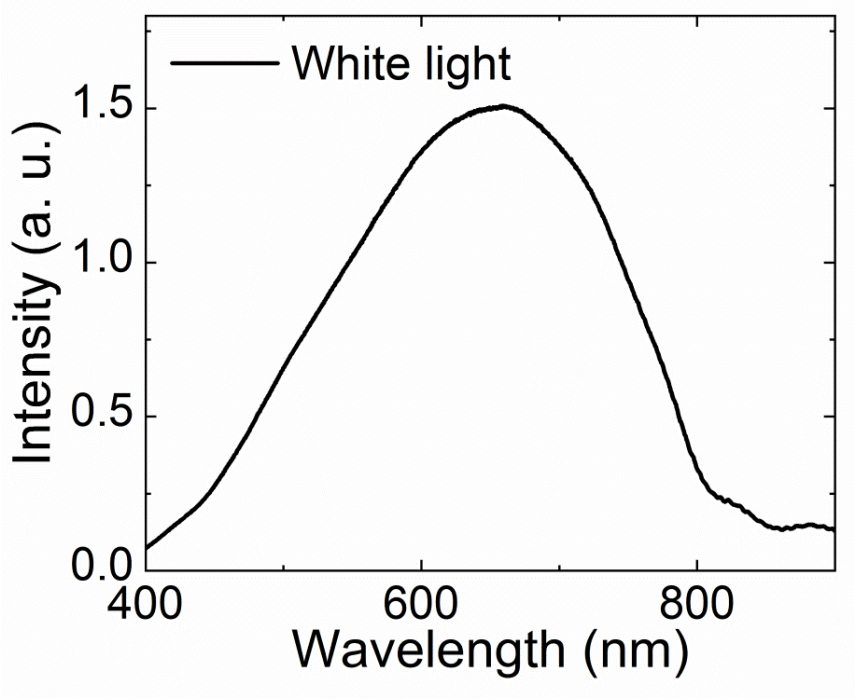

Figure S6. Spectrum of the halogen lamp used in the measurements of the reflection spectra.

Supplementary Note 7: Numerical simulations of reflection spectra

The numerical simulations of the reflection spectra were carried out by using the finite-difference time-domain (FDTD) method. The thicknesses of the bottom Au film and the polymer film were chosen to be 100 and 80, respectively. For simplicity, we considered only the evolvement of closely-packed Au nanoislands into elliptical Au nanoparticles upon the irradiation of femtosecond laser light, as schematically illustrated in Figure S7A. The regulation of disordered Au nanoparticles into a nanograting, which is composed of regularly arranged Au nanoparticles, is taken into account by using a periodic boundary condition in the numerical simulations. As depicted in Figure S7A, it is assumed that a nanodisk (the initial shape of nanoislands) is transformed into a nanosphere after melting at small laser fluence. With increasing laser fluence, the nanosphere is further reshaped into an ellipsoid at high laser fluence. The volume of the nanoparticle remains unchanged during the transformation. Since the diameter and height of the nanodisk were chosen to be 80 and 20 nm, the diameter of the nanosphere was derived to be ~50 nm. The reshaping of the nanosphere into ellipsoid was modeled by decreasing that in the *x* direction and increasing the dimension in the *y* direction. The dimension in the z direction was changed accordingly to keep the same volume of the nanoparticle. The dimensions of the ellipsoid in the final stage were estimated to be 40, 70, and 24 nm in the *x*, *y*, and *z* directions. A plane wave polarized along the *x* direction was normally incident on the nanograting and the spectra of the reflected light were recorded by using a monitor on top of the nanograting. In Figure S7B, we compared the reflection spectra calculated by using the numerical simulations and those obtained in the optical measurements. Although the physical model we used is quite simple, a qualitative agreement between the simulated and measured results is observed.

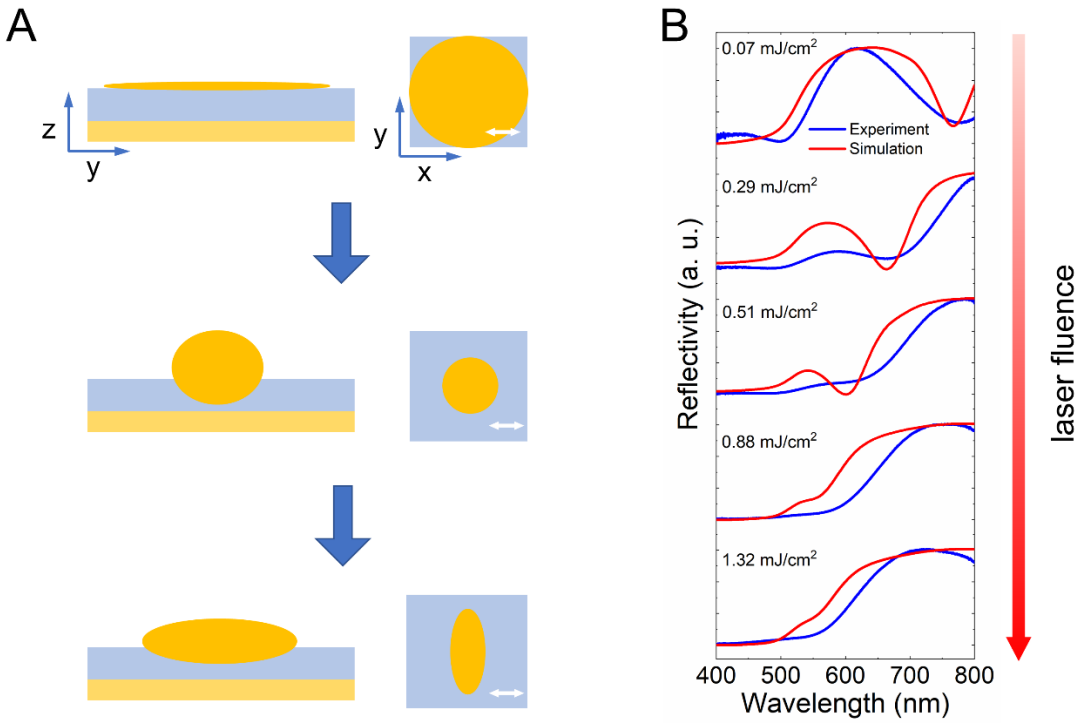

Figure S7. (A) Schematic showing the melting of Au nanoislands and the elongation of Au nanoparticles induced by femtosecond laser light with increasing fluence. (B) Reflection spectra measured and calculated for Au nanoislands after irradiation of femtosecond laser light.

Supplementary Note 8: Nanogratings formed in the thin polymer (PMMA) film

As we have shown in the main text, nanogratings composed of regularly arranged elliptical Au nanoparticles were created on top of the thin polymer (PMMA) film after irradiating closely-packed Au nanoislands with femtosecond laser light with a sufficiently large fluence. In our experiments, we also examined the surface morphology of the polymer film by removing the surface nanograting by using SEM observations, as shown in Figure S8. It is noticed that periodic ripples (a kind of nanograting) were created on the surface of the polymer. In each case, the orientation of the nanograting, which is indicated by parallel yellow lines, is perpendicular to the polarization of the laser light. This feature is also reflected in the Fourier transformations of the SEM images, which are shown as insets. In all cases, the periodicity of the nanograting was extracted to be ~80 from the Fourier transformations of the SEM images, quite similar to that of the nanograting composed of Au nanoparticles.

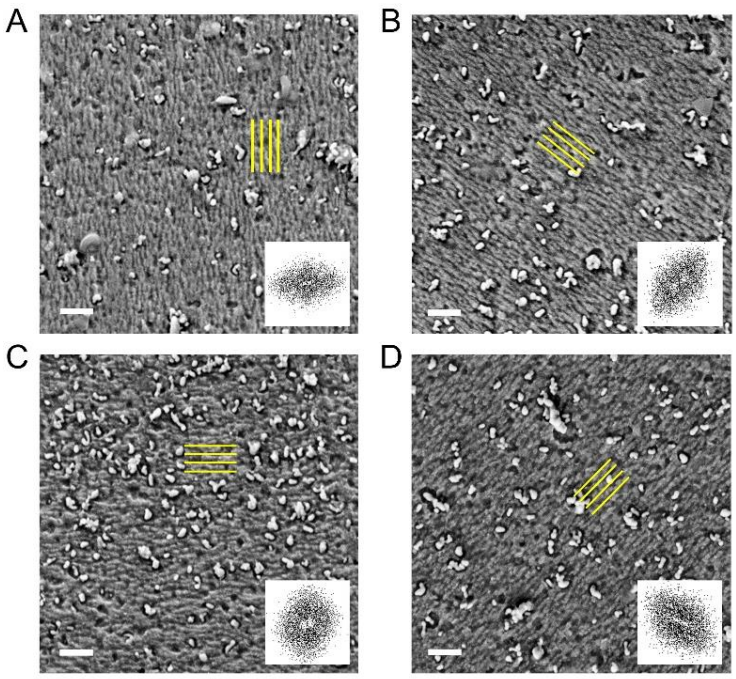

Figure S8. SEM images of the nanogratings induced in the thin polymer (PMMA) film by using femtosecond laser light with a polarization angle of θ = 0° (A), θ = 45° (B), θ = 90° (C), and θ = 135° (D). In each case, the Fourier transformation of the image indicating the orientation direction of the polymer nanograting is shown in the inset. The length of the scale bar is 300 nm.

Supplementary Note 9: Calculation of the efficacy factors characterizing the interaction between a rough Au film with femtosecond laser light

Physically, the interaction of a metal surface with femtosecond laser light and the laser-induced periodic surface structures (LIPPSs) can be described by the theory proposed in Ref. 13. The interference between the incident light and the scattering light from the rough surface (or the surface plasmon wave) is considered as the physical origin for the formation of LIPPSs. Based on this theory, the interaction of the rough metal surface with femtosecond laser light can be characterized by the so-called efficacy factor, which is determined by the dielectric constant of the metal and two parameters named as shape and filling factors (denoted as s and f in the following). We simulated the dependence of the efficacy factor as functions of the normalized wavelength κ_x and κ_y, which are defined as $\kappa_x = \lambda/\Lambda_x$, $\kappa_y = \lambda/\Lambda_y$ (here, λ is the wavelength of the laser light, Λ_x

and Λ_y are the periods of the LIPSSs along the x and y directions), for different values of s and f, as shown in Figure S9. For linearly polarized light along the x direction, one can see maximum values of the efficacy factor at $\kappa_y = \pm 1$, implying the preferential formation of LIPSSs with a period close to the laser wavelength in the direction perpendicular to the laser polarization (x direction). This kind of LIPSSs belongs to low-frequency LIPPSs which is commonly observed on the surface of a metal film irradiated by using femtosecond laser light. However, we did not find any maxima of the efficacy factor at larger κ_x and κ_y, implying the absence of high-frequency LIPSSs. This result indicates that the interference model mentioned above is too simple to predict the formation of high-frequency LIPSSs, which is caused by complicated physical mechanisms, as indicated previously in Ref. 8.

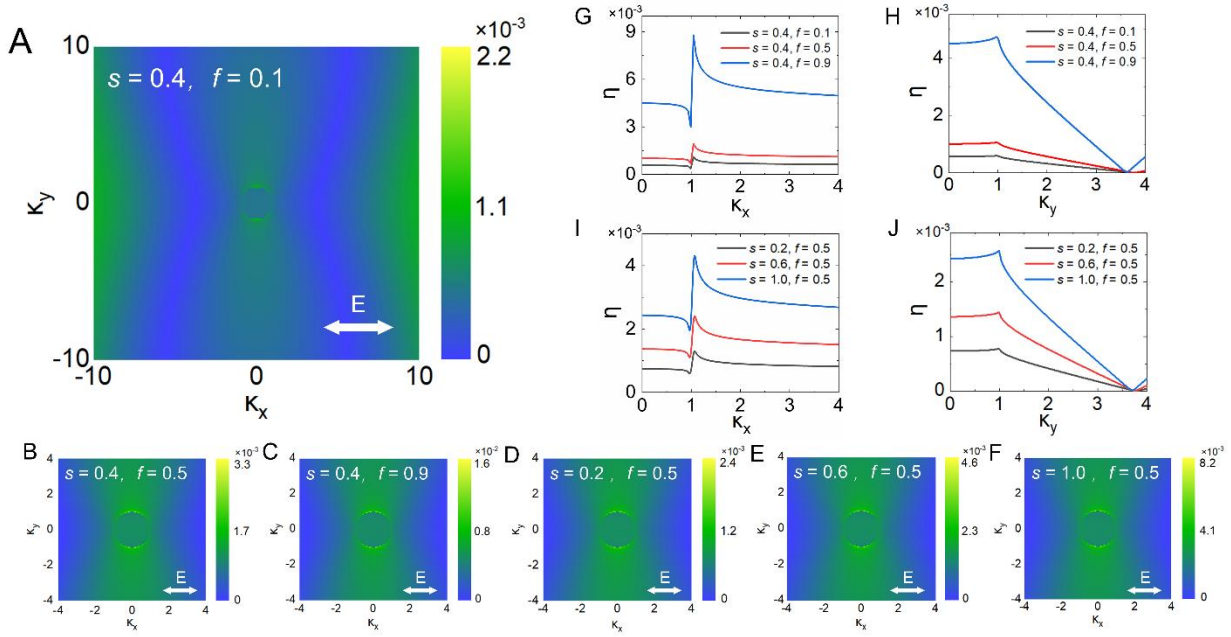

Figure S9. Two-dimensional (A-F) and one-dimensional (G-J) plots of the efficacy factors as functions of the normalized wavelengths calculated for a rough Au film with different shape and filling factors based on the simple model proposed in Ref. 13.

Supplementary Note 10: Dependence of the polarization state of the reflected light on that of the incident light

In Figure S10A,B, we present the polarization states of the reflected light at different wavelengths ranging from 480 to 740 nm for the incident light with polarization angles of 135°

and 120° with respect to the vector of the nanograting fabricated by using femtosecond laser light with a polarization angle of $\theta = 0°$. The polarization states of the reflect light at shorter wavelength ranging from 500 to 600 nm are shown in Figure S10C,D, respectively. For the incident light with a polarization angle of α = 135°, the reflected light appears to be circularly polarized at 660 nm and it evolves gradually to an elliptically polarized light and linearly polarized light. The polarization state is rotated towards the vector of the nanograting with increasing wavelength. At a longer wavelength of 740 nm, polarization angle is reduced to be $\alpha = 20°$. For the incident light with a polarization angle of α = 120°, the rotation of the polarization state of the reflected light at long wavelengths towards the vector of the nanograting is still observed. However, a larger polarization angle of $\alpha \sim 30°$ is observed at 740 nm.

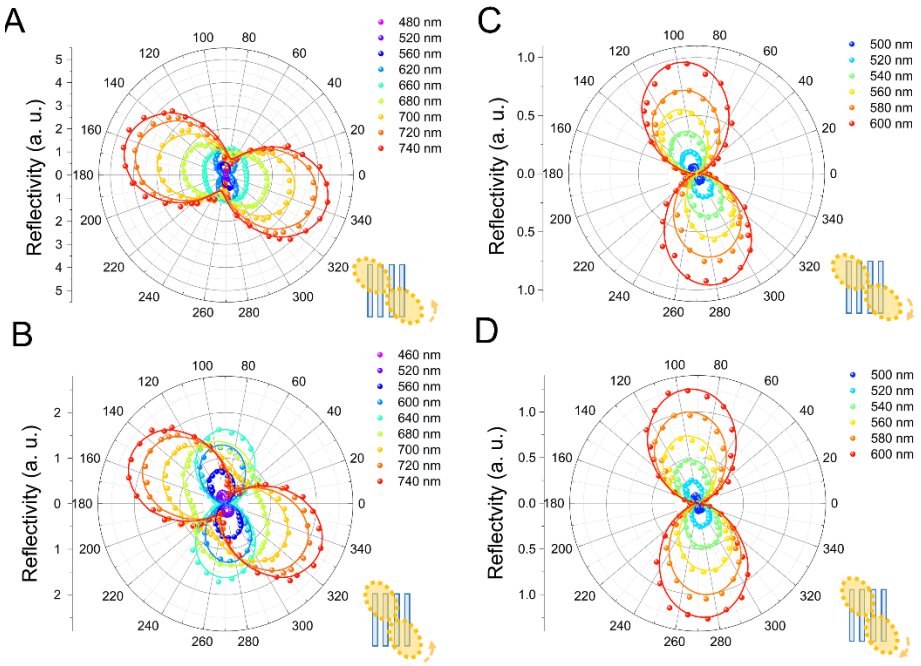

Figure S10. Polarization states of the reflected light measured for No. 7 flower, which was recorded by using femtosecond laser light with $\theta = 0°$, at different wavelengths ranging from 480 to 740 nm. The flower was illuminated by using polarized white light with $\alpha = 135°$ (A) and $\alpha = 120°$ (B). The enlarged polarization states at shorter wavelengths ranging from 500 to 600 nm are shown in (C) and (D), respectively. In each case, the orientation and vector of the nanograting are presented in the inset.

Supplementary Note 11: Extracting the recorded polarization state

In Figure S11, we present the experimental results for imprinting the polarization states of the femtosecond laser light with nanogratings. The polarization states of the femtosecond laser light were recorded in different characters of Science & Technology with an increment of 10°. Two polarizers with cross polarization were employed to extract the polarization states imprinted in nanogratings. The pixel sizes were chosen to be 0.50 μm. The thinnest parts of some characters include only one pixel.

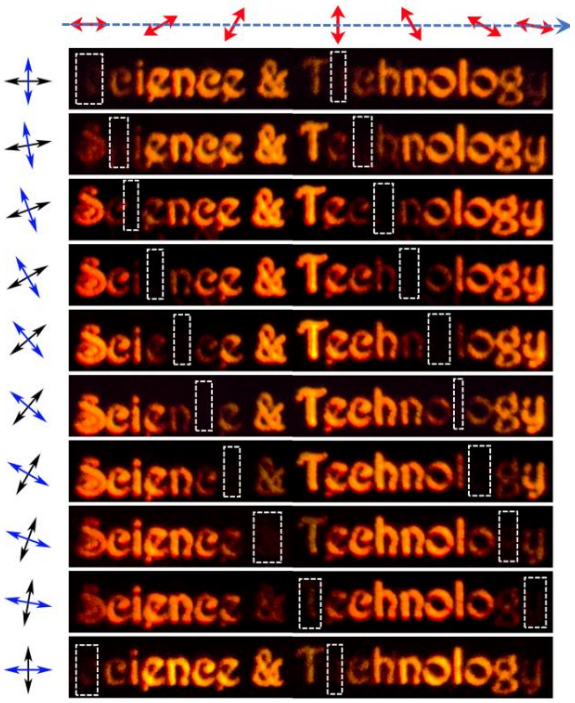

Figure S11. Recording of the polarization states of femtosecond laser light into different characters of Science & Technology with an increment of 10° and a pixel size of 0.50 μm.

Supplementary Note 12: Parameters of femtosecond laser light used to record the flower/leaf and school logo

In order to show the polarization sensitive structural colors exhibited by the nanogratings induced by using femtosecond laser light, we designed a pattern composed of flowers and leaves

(see Figure S12A) and created the structural colors by using femtosecond laser light with different wavelengths, polarizations and fluence, as shown in Figure S12B. The detailed parameters of the femtosecond laser light used to generate the structural colors are listed in Table S1. Also, we used the structural colors generated by using femtosecond laser light with different parameters to decorate the logo of our school, as shown in Figure S12C. Accordingly, the detailed parameters of the femtosecond laser light are listed in Table S2.

Table S1. Detailed parameters of the femtosecond laser light used to create the colorful flowers and leaves.

Item	**1**	**2**	**3**	**4**	**5**	**6**	**7**	**8**	**9**	**10**	**11**	**12**	**13**
Wavelength (nm)	800	800	750	750	800	750	750	750	750	800	850	750	750
Polarization angle (°)	90	90	90	90	90	90	0	0	135	0	0	0	45
fluence values (mJ/cm^2) Leaf /Petal	0.73	0.73	0.95	1.25	0.59	1.47	1.47	1.17	0.93	0.59	2.42	0.37	0.95
fluence values (mJ/cm^2) Vein /Stamen	0.95	0.95	1.25	1.61	0.95	1.83	1.83	1.39	1.17	0.88	0.73	0.59	1.17

Table S2. Detailed parameters of the femtosecond laser light used to create the colorful school logo.

Item	**1**	**2**	**3**	**4**	**5**	**6**	**7**	**8**	**9**	**10**	**11**	**12**	**13**	**14**	**15**	**16**
Wavelength (nm)	750	750	750	750	750	750	750	750	750	750	750	750	750	750	750	750
Polarization angle (°)	135	45	0	90	0	90	0	0	0	0	0	0	0	0	0	45
fluence values (mJ/cm^2)	1.32	1.10	0.51	103	0.59	1.10	1.17	0.07	0.22	0.37	0.51	0.66	0.88	1.10	1.32	0.73

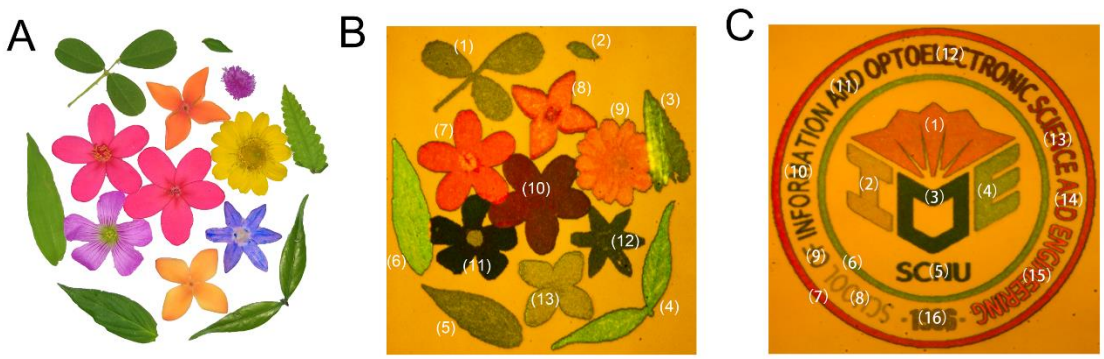

Figure S12. (A) Designed pattern composed of flowers and leaves. Colorful flower/leaf (B) and school logo (C) patterns created by using femtosecond laser light with different parameters (polarization, wavelength and fluence).

Supplementary Note 13: Dependence of the structural color on the polarization of the incident light

In order to examine the sensitivity of the structural color exhibited by the fabricated nanograting on the polarization of the incident light, we took the pictures of the flower/leaf illuminated by using polarized white light with different polarization angles (with an increment of 5°) under a reflective microscope, as shown in Figure S13.

Figure S13. Structural colors exhibited by the flower/leaf patterns illuminated by using polarized white light with different polarization angles.

Supplementary Note 14: Effect of the polymer film thickness on the generation of structural color

In Figure S14A, we show the two-dimensional plot of the reflectivity as functions of wavelength and polymer film thickness. For femtosecond laser light whose wavelength is tunable in the range of 700–850 nm, a low reflectivity, which implies an effective interaction of Au nanoislands with the femtosecond laser light, is available only for polymer film thickness in the range of 60–140

nm. This feature provides a guideline for designing the thickness of the polymer film in our samples. Otherwise, no abundant structural colors can be generated, as shown in Figure S14B.

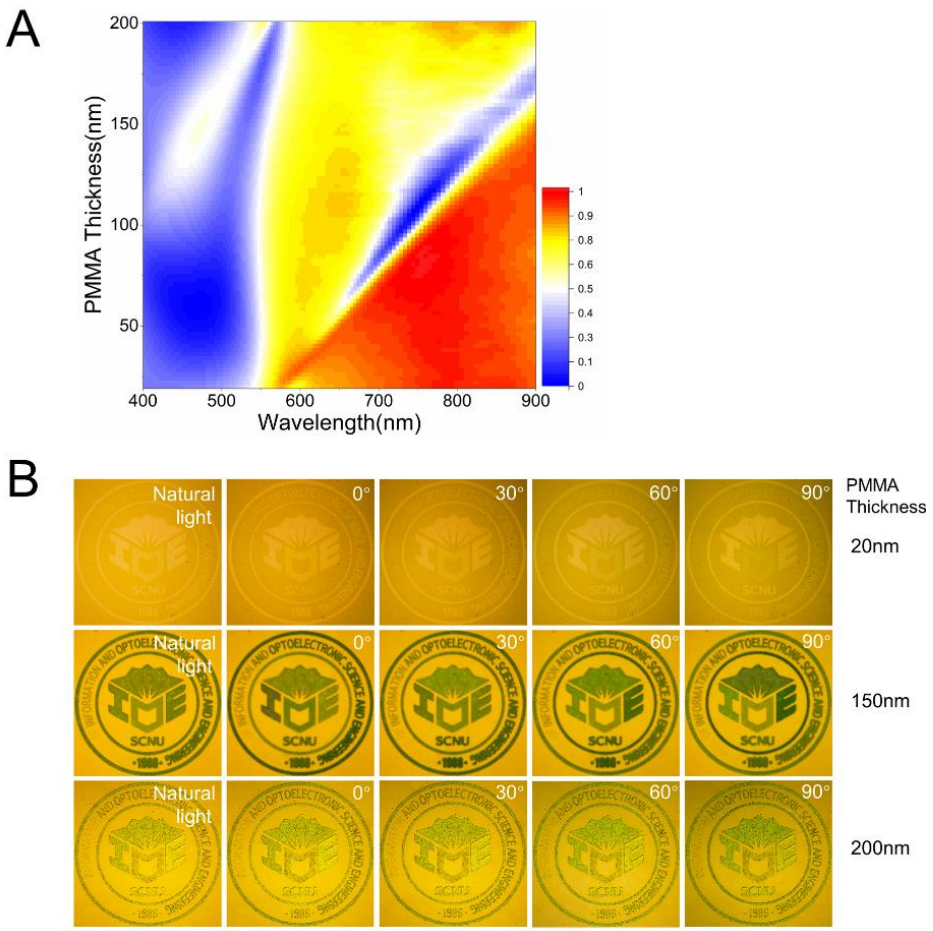

Figure S14. (A) Two-dimensional plot of the reflectivity of the sample as functions of wavelength and polymer film thickness. (B) Structural colors exhibited by the samples with different polymer film thicknesses of d = 20, 150 and 200 nm under the illumination of unpolarized and polarized white light.

Supplementary Note 15: Images observed by using oblique incidence light

We also examined the recorded pattern illuminated by using an oblique incidence light, as shown in Figure S15A. The image observed by using a normal incidence light is provided for comparison. It is noticed that the structural colors exhibited by the nanogratings in the case of normal incidence disappear completely when oblique incidence light was employed. This behavior can be easily

understood because the structural colors in our case originate from the interference of the partial reflected waves from a particle-on-film system, where the polymer film in between the metallic nanoparticles and the metal film plays a crucial role in determining the reflection spectra. When oblique incidence light was employed, we observed the scattered light from metallic nanoparticles instead of the reflected light from the whole system.

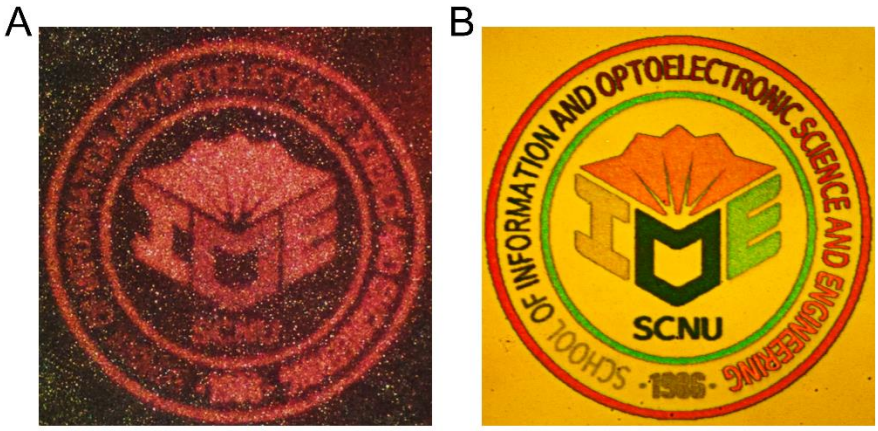

Figure S15. Images observed under the bright-field microscope with oblique (A) and normal (B) incidence beam.

Supplementary Note 16: Influence of the pixel size on the structural color

Apart from the parameters of the femtosecond laser light used to create nanogratings and the thickness of the polymer film, the pixel size of the recorded pattern also has influence on the structural color, as shown in Figure S16.

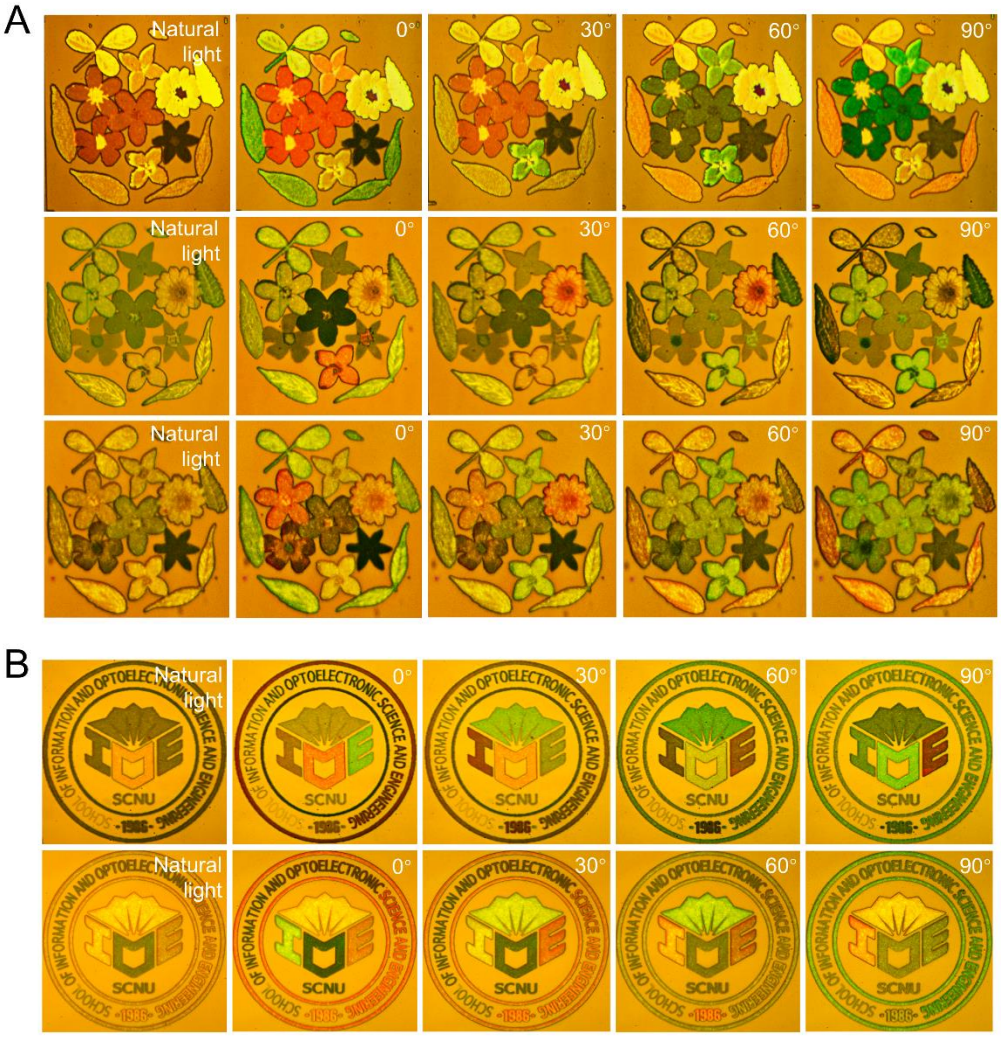

Figure S16. (a) Structural colors exhibited by the flower recorded by using different pixel sizes of 1.0 μm (300 × 300 pixels, 1st row), 0.5 μm (600 × 600 pixels, 2nd row), and 0.4 μm (600 × 600 pixels, 3rd row) and observed by using unpolarized (1st column) and polarized white light with polarization angles of 0° (2nd column), 30° (3rd column), 60° (4th column), and 90° (5th column). (b) Structural colors exhibited by the school logo recorded by using different pixel sizes of 0.7 μm (400 × 400 pixels, 1st row) and 0.4 μm (600 × 600 pixels, 2nd row) and observed by using unpolarized (1st column) and polarized white light with polarization angles of 0° (2nd column), 30° (3rd column), 60° (4th column), and 90° (5th column).

Supplementary Note 17: Structural color generated by using continuous wave laser light

In Figure S17, we present the structural colors generated by using continuous wave laser light (unlocked output of femtosecond laser light). In this case, we did not observe abundant structural colors as we did when using femtosecond laser light. Only two structural colors, namely brown and green, were observed at low and high laser fluence, respectively.

Figure S17. Colorful school logo created by using continuous wave laser light at 750 nm and observed by using unpolarized (1st column) and polarized white light with polarization angles of 0° (2nd column), 30° (3rd column), 60° (4th column), and 90° (5th column).